Eley−Rideal Dynamics of the Chlorine Atom Abstraction of Hydrogen Chemisorbed on Silicon

W. K. Kim,† J. Ree,† and H. K. Shin*

Department of Chemistry,‡ University of Nevada, Reno, Nevada 89557

Received: July 9, 1998; In Final Form: September 28, 1998

The reaction probability and product-state energy distribution in the Eley−Rideal reaction of gas-phase atomic chlorine with hydrogen atoms chemisorbed on a silicon surface are studied by use of the classical trajectory approach. Our model for study is based on reaction zone atoms interacting with a finite number of primary-system silicon atoms, which are coupled to the heat bath. At a gas temperature of 1500 K and a surface temperature of 300 K, all reactive events occur on a subpicosecond time scale as a result of efficient energy flow from the gas atom to the adatom−surface bond. These events are localized around the adatom site on the surface. Most of the reaction exothermicity is deposited into the translational and vibrational motions of HCl, producing a non-Boltzmann distribution. The reaction probability increases rapidly as the gas temperature is raised from 300 to 1000 K, above which it remains nearly constant at about 0.18. All product molecules leaving the surface undergo a cartwheel-like rotation.

I. Introduction

The chemisorption of hydrogen atoms on a silicon surface occurs during gas−surface reactions, such as chemical vapor deposition from silane, and the reactivity of these adatoms is of major importance in understanding silicon-surface-assisted processes.[1−7] One such process is the abstraction of adatoms by incident gas atoms, such as hydrogen or halogen atoms, in which case the reaction probability and product energy distribution are among the important problems to be studied. The problem of chlorine atoms interacting with chemisorbed hydrogen atoms is particularly important, since these atoms are involved in etching processes. In such gas−adatom interactions, the reaction is initiated by the incidence of gas-phase atoms, which are initially not in equilibrium with the surface. Therefore, the resulting reactive events in this collision-induced process may follow the Eley−Rideal (ER) mechanism. The ER mechanism has been considered to be much less common than the Langmuir−Hinshelwood (LH) type,[8] but recent experiments[2−4,7−12] and calculations[13−24] show evidence of a number of gas atom−adatom reactions occurring through the ER mechanism. A mechanism that is between these classic types is the hot precursor mechanism in which gas atoms are trapped in the neighborhood of the surface but have not thermalized.[25,26] In the Cl(g) + H(ad)/Si reaction, the H−Cl bond energy is about 4.4 eV. The adsorption energy of an H atom on Si(001) is 3.5 eV, and the adsorption energy of a Cl atom with Si(001) is 3.7 eV. Thus, the exothermicity suggests that the HCl formation is likely to follow the ER mechanism. On the other hand, the LH step can play an important role in a reaction where the sum of adsorption energies is close to but less than the bond energy. For example, in H(g) + Cl(ad)/Au(111), the Cl−Au and H−Au adsorption energies are about 2 eV.[27,28] In this case, the LH reaction of HCl is approximately thermoneutral and its contribution to the overall reaction can be important.[28]

The purpose of this paper is to study the ER reaction of gas-phase atomic chlorine with chemisorbed hydrogen atoms on silicon (001)−(2 × 1) with particular reference to the problem of product energy distribution. For this purpose, we shall determine the extent of reaction by following the time evolution of the pertinent coordinates and conjugate momenta of each trajectory on a potential energy surface constructed with many-body interactions operating between all atoms of the reaction system. The time evolution will be determined by solution of the equations of motion formulated by uniting gas−surface dynamics procedure and generalized Langevin theory for the solid phase.[22,29,30] In this collision-induced process, the dynamics of energy flow between the gas atom and the adatom−surface vibration is a problem of fundamental importance in understanding the details of reactive events that follow, thus determining the extent of reaction and product energy distribution. We consider the reaction, which takes place at a gas temperature of 1500 K and a surface temperature of 300 K. A brief discussion of the temperature dependence of reaction will be presented.

II. Interaction Model and Energies

The interaction model and numerical procedures have already been reported in ref 24. We recapitulate the essential aspects of the interaction on the silicon (001)−(2 × 1) surface reconstructed by forming dimers along the [110] direction (Figure 1a). For ready reference we have displayed the collision model in Figure 1b, which is the same as that in ref 24 except that the hydrogen and chlorine atoms are interchanged. The H atom is chemisorbed on the Si atom of the symmetric dimer structure. This Si atom is the 0th member of the $(N + 1)$-atom chain that links the reaction zone to the heat bath, providing a simple quasiphysical picture of energy flow between the reaction zone and the chain atoms and, in turn, between the chain and the heat bath. (Here, $N + 1$ signifies the 0th Si atom plus N atoms of the chain.) Through this coupling, the heat bath exerts systematic dissipative and random (or stochastic) forces on the primary system composed of the reaction zone atoms and the

* To whom correspondence should be addressed.
† Permanent address: Department of Chemistry Education, Chonnam National University, Kwangju, Korea.
‡ Theoretical Chemistry Group Contribution No. 1167.

10.1021/jp982927f CCC: $18.00
Published on Web 01/21/1999

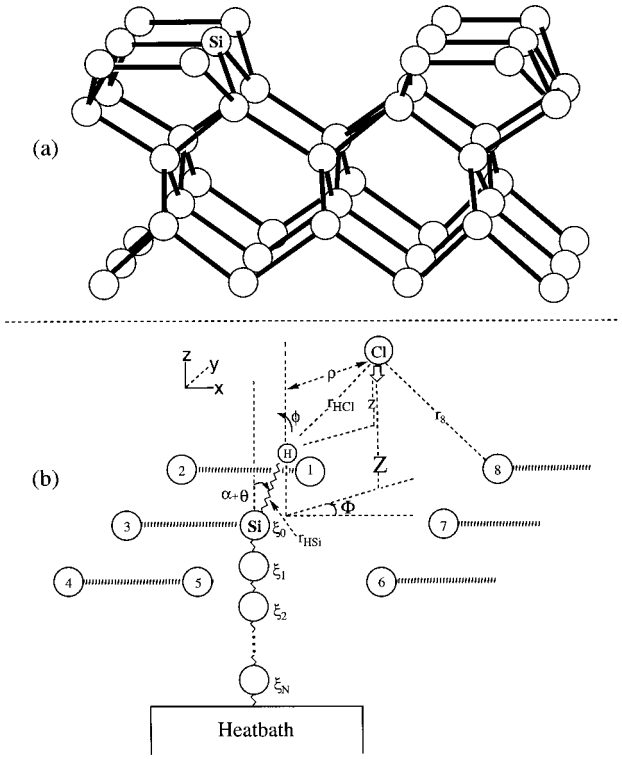

Figure 1. (a) Symmetric Si−Si dimer surface. (b) Interaction model showing the H atom adsorbed on the surface adsorption site indicated by "Si", the 0th atom, which is coupled to the *N*-atom chain. The *N*th atom of the chain is coupled to the heat bath. The position of H is described by (r_{HSi},θ,ϕ), and the position of Cl by (ρ,Z,Φ). α is the tilt angle. The Cl to H is denoted by r_{HCl} and the Cl-to-the-*i*th surface-layer Si atom by r_i. The coordinates of the (N + 1) chain atoms including the 0th atom are denoted by ξ_0, ξ_1, ..., ξ_N.

N-chain atoms. The reaction zone atoms are the 0th Si atom, the adatom, and the incident Cl gas atom. We consider that these reaction zone atoms and the *N*-chain atoms constitute the primary system. We then designate the remaining infinite number of solid atoms as secondary atoms.

The reaction occurs through the strong interaction of the chlorine atom with the adatom, forming a loosely bound complex Cl···H−Si during the collision, and the essential aspect of the reactive event can be described in terms of the interactions of these (N + 1) + 2 atoms. Although the energy of these interactions is of primary importance in determining the extent of reaction, the potential energies resulting from the nearby Si atoms that surround the 0th Si atom can affect the outcome of the collision event. These nearby surface-layer atoms can enhance the attraction of the gas atom to the surface site through their long-range attractive forces and can then form a repulsive wall when the gas atom approaches too close to the surface. Consideration of such interactions is appropriate for the interaction of surface atoms with the gas atom, which is loosely bound to the adatom. Furthermore, such a model is also an appropriate procedure in describing the surface fully covered with adatoms. Thus, in the present model, the surface-layer atoms can steer the loosely bound gas atom to remain in the neighborhood of the adatom during the reaction, thus affecting the outcome of collision. In the model, we consider the 0th Si atom of the chain to be surrounded by eight nearby Si atoms of the symmetric dimer strands,[24] and we include the resulting interactions between them and the gas atom in constructing the potential energy surface (PES). In this model, we consider only one hydrogen atom on top of the 0th Si atom, the state that has been shown to be of major importance over the dihydrogenated or trihydrogenated cases.[4,31] The initial state is chosen to be that of the gas atom incident normal to the surface with the initial collision energy E and impact parameter b.

A total of six degrees of freedom is needed to describe the motions of Cl and H atoms above the surface. Although it is straightforward to transform these coordinates to the center-of-mass and relative coordinate systems, we find it convenient to describe the collision system including surface atoms in terms of the atomic coordinates H(x_H,y_H,z_H) and Cl(x_{Cl},y_{Cl},z_{Cl}). The H coordinates are

$$x_H = r_{HSi} \sin(\alpha + \theta) \cos \phi$$

$$y_H = r_{HSi} \sin(\alpha + \theta) \sin \phi$$

and

$$z_H = r_{HSi} \cos(\alpha + \theta), \quad \text{i.e.,} \quad H(x_H,y_H,z_H) = H(r_{HSi},\theta,\phi)$$

Prior to dissociation, the adatom tilted at an angle of $\alpha = 20.6°$ [32] undergoes hindered motions along θ and ϕ. For the position of Cl with respect to the reference axis along the adatom, the Cl−H interatomic distance r_{HCl} is $(\rho^2 + z^2)^{1/2}$, where ρ is the distance between Cl and the H-surface normal axis and z is the vertical distance from Cl to the horizontal line determining the position of H. Note that the initial ($t \rightarrow -\infty$) value of ρ is the impact parameter b. The projection of r_{HCl} on the surface plane is oriented by the angle Φ from the X axis. Thus, the coordinate (x_{Cl},y_{Cl},z_{Cl}) can be transformed into the cylindrical system (ρ,Z,Φ), where Z is the Cl-to-surface distance. The vertical distance z is then

$$z = Z - r_{HSi} \cos(\alpha + \theta)$$

Thus, the occurrence of reactive events can be determined by studying the time evolution of the H−Si bond distance r_{HSi} and the Cl-to-H distance $r_{HCl} = (\rho^2 + z^2)^{1/2}$ for the ensemble of gas atoms approaching the surface from all directions. Any rigorous form of the interaction potential should include all those interactions mentioned above. For the overall interaction energy, we combine a modified form of the London−Eyring−Polanyi−Sato (LEPS) potential energy surface[24] for the interactions of Cl to H, H to Si, and Cl to nine surface-layer atoms, all of which are considered to be exponential, with the θ- and ϕ-hindered rotational motions and the harmonic motions of the (N + 1)-chain atoms:

$$U = \{Q_{HCl} + Q_{HSi} + Q_{ClSi} - [A_{HCl}{}^2 + A_{Hsi}{}^2 + A_{ClSi}{}^2 - A_{HCl}A_{HSi} - (A_{HCl} + A_{HSi})A_{ClSi}]^{1/2}\} + \frac{1}{2}k_\theta(\theta - \theta_e)^2 + \frac{1}{2}k_\phi(\phi - \phi_e)^2 + \sum_j \left(\frac{1}{2}M_s\omega_{ej}{}^2\xi_j{}^2\right) + \sum_j \left(\text{terms of type } \frac{1}{2}M_s\omega_{cj}{}^2\xi_{j-1}\xi_j, \frac{1}{2}M_s\omega_{c,j+1}{}^2\xi_j\xi_{j+1}, \text{ etc.}\right) \quad (1)$$

where k_θ and k_ϕ are force constants, θ_e and ϕ_e are the equilibrium angles, M_s is the mass of the silicon atom, ω_{ej} is the Einstein frequency, and ω_{cj} is the coupling frequency characterizing the chain. The explicit forms of the Coulomb term (Q's) and exchange terms (A's) for HCl, HSi, and ClSi are given in ref 24. Since $r_i \equiv r_i(r_{HSi},\theta,\phi,\rho,Z,\Phi)$ and $r_{HCl} \equiv r_{HCl}(r_{HSi},\theta,\rho,Z)$, the potential energy surface has the functional dependence of $U(r_{HSi},\theta,\phi,\rho,Z,\Phi,\{\xi\})$, where $\{\xi\} = (\xi_0, \xi_1, ..., \xi_N)$ for the vibrational coordinates of the (N + 1)-chain atoms.

The potential and spectroscopic constants for the H−Cl and H−Si interactions are[33] $D^0_{0,HCl} = 4.434$ eV, $D^0_{0,HSi} = 3.50$ eV,[34,35] $a_{HCl} = 0.268$ Å, $a_{HSi} = 0.334$ Å, $\omega_{HCl}/(2\pi c) = 2990.95$ cm^{-1}, and $\omega_{HSi}/(2\pi c) = 2093$ cm^{-1},[15,36] where a's are exponential range parameters determined from the relation $a = (D_i/(2\mu_i))^{1/2}/\omega_i$ for $i =$ HCl or HSi.[24] The well-depth constants that enter in the Coulomb and exchange terms for H−Cl and H−Si are determined as $D_{HCl} = D^0_{0,HCl} + (1/2)\hbar\omega_{HCl}$ and $D_{HSi} = D^0_{0,HSi} + (1/2)\hbar\omega_{HSi}$, respectively. The equilibrium distances (d) of the H−Cl and H−Si bonds are 1.274 and 1.514 Å, respectively. For the x- and y-directions, vibrational energies $\hbar\omega_{HSi,x}$ and $\hbar\omega_{HSi,y}$ of the H atom chemisorbed on Si are 645 cm^{-1}, whereas the z-direction vibrational energy is 2093 cm^{-1}.[15,36] The force constant describing the hindered motion in the x (or y) direction is determined as $k = \mu_{HSi}(\omega_{HSi,x}d_{HSi})^2 = 3.537$ eV.

During the collision, the incident gas atom becomes loosely bound to the adatom (i.e., Cl···H−Si) in the Cl(p_z)−H(s) bonding state and experiences the interaction coming from nearby surface-layer atoms. The overlap of the p_x or p_y orbital of Cl with the atomic orbitals of adjacent Si atoms is not efficient. This nonbonding character of p_x or p_y leads to Pauli repulsion for the back-wall of the physisorption interaction, with van der Waals energy representing the attractive branch. Then the interaction between the Cl and the surface-layer atoms can be characterized by a small value of well depth and can be include in the Q_{ClSi} and A_{ClSi} of the LEPS potential. There is no data on the interaction of such a bound gas atom with the Si surface, but the well depth is not expected to be significantly different from 100 meV.[37−39] We can estimate it assuming the ratio $D_{diatom/surface}/D_{atom/surface} = 1.2$.[37] For a number of diatomic and small polyatomic molecules on the related system of the graphite surface, the well depth is in the range 100−150 meV.[37] We assume the value of $D_{diatom/surface}$ to fall in this range and take its value to be 125 meV; thus, the energy term $D_{atom/surface}$ can be estimated as 104 meV. We also take $a_{ClSi} = 0.35$ Å to reflect the characteristics of physisorption. The determination of the equilibrium distances between Cl and the adjacent surface atoms is tedious but is straightforward. For example, for $b = 0$ the distance between Cl and the 0th Si atom is 2.74 Å. The distance between Cl and the nearest atom (3rd in Figure 1b) is 4.07 Å, the distance between Cl and the next-nearest atom (2nd or 4th) is 4.50 Å, the distance between Cl and the next-next-nearest atom (1st or 5th) is 4.74 Å, etc.

By varying values of Δ's systematically, we find the set of Sato parameters best describing the desired features minimizing barrier height and attractive well in the product channel to be $\Delta_{ClH} = 0.30$, $\Delta_{HSi} = -0.10$, $\Delta_{ClS} = 0.40$ for the reaction zone Si atom (i.e., the Cl to 0th Si atom) and $\Delta_{ClS} = 0.20$ for the Cl to remaining eight surface-layer Si atoms. For this reaction, the activation energy is known to be only 2.1 ± 0.2 kcal/mol.[2,18]

III. Calculations and Discussion

Once the PES is determined, we can follow the time evolution of the primary system by integrating the equations, which describe the motions of the reaction-zone atoms and N-chain atoms included in the model. We expect that this PES will enable us to understand how gas atoms with given initial conditions react with chemisorbed atoms and then desorb from the surface. An intuitive way to treat the dynamics of the reaction involving many surface atoms is to solve a united set of equations of motion for the reaction-zone atoms and the Langevin equation for N-chain atoms, which couples the primary system to the heat bath. The gas−adatom part of the resulting equations are $m_i\ddot{Q}_i(t) = -\partial U/\partial Q_i$, where $Q_1 = Z$, $Q_2 = \rho$, $Q_3 = \Phi$, $Q_4 = z_{HSi}$, $Q_5 = \theta$, and $Q_6 = \phi$, with $m_1 = \mu_{Cl}$, $m_2 = \mu_{HCl}$, $m_3 = I_{HCl}$, the moment of inertia, $m_4 = \mu_{HSi}$, and $m_5 = m_6 = I_{HSi}$. Here, μ_i is the reduced mass of the interaction system indicated. For the $(N+1)$-atom chain, which includes the 0th Si atom, the equations are[24,29]

$$M_s\ddot{\xi}_0(t) = -M_s\omega_{e0}{}^2\xi_0(t) + M_s\omega_{cl}{}^2\xi_1(t) - \partial U_{LEPS}(z_{ClSi},\theta,\phi,\rho,Z,\Phi,\{\xi\})/\partial\xi_0 \quad (2a)$$

$$M_s\ddot{\xi}_j(t) = -M_s\omega_{ej}{}^2\xi_j(t) + M_s\omega_{cj}{}^2\xi_{j-1}(t) + M_s\omega_{c,j+1}{}^2\xi_{j+1}(t), \quad j = 1, 2, ..., N-1 \quad (2b)$$

$$M_s\ddot{\xi}_N(t) = -M_s\Omega_N{}^2\xi_N(t) + M_s\omega_{c,N}{}^2\xi_{N-1}(t) - M_s\beta_{N+1}\dot{\xi}_N(t) + M_sf_{N+1}(t) \quad (2c)$$

Equation 2a is for the vibration of the 0th chain atom on which the H atom is chemisorbed. In this equation, we only take the ξ_0 derivative of the LEPS part (i.e., the first part) of eq 1, since the derivatives of the harmonic and coupling terms appearing in the sums are already given by the first two terms of eq 2a. Equation 2c is for the vibration of the Nth atom, which is bound to the bulk phase. In this equation, Ω_N is the adiabatic frequency. That is, at short times the jth oscillator responds like an isolated harmonic oscillator with frequency ω_{ej}, whereas Ω_N determines the long-time response of the heat bath. The friction coefficient β_{N+1} is very close to $\pi\omega_D/6$, where ω_D is the Debye frequency, and governs the dissipation of energy from the primary zone to the heat bath. All values of β and those of ω_e, ω_c, and Ω are presented elsewhere.[21] The quantity $M_sf_{N+1}(t)$ is the random force on the primary system arising from thermal fluctuation in the heat bath. This force balances, on average, the dissipative force, $M_s\beta_{N+1}\dot{\xi}_N(t)$, which removes energy from the primary system in order that the equilibrium distribution of energies in the primary system can be restored after collision. The random force term is white noise, whose fluctuations are governed by a Markovian fluctuation−dissipation theorem $\langle f_{N+1}(t)f_{N+1}(0)\rangle = (6kT_s/M_s)\beta_{N+1}\delta(t)$.[29] Short-time reactive events are not affected by these long-time response and dissipation terms. Thus, if we ignore these dissipation and stochastic terms and replace Ω_N by ω_{eN} in eq 2c, we have a set of equations for studying the typical short-time processes of the interaction between the incident atom and an atom bound to an $(N+1)$-atom cluster.

The computational procedures include an extensive use of Monte Carlo routines to generate random numbers for initial conditions. The first of them is to sample collision energies E from a Maxwell distribution at the gas temperature T_g. We sample 30 000 values of E. In sampling impact parameters b, we note that the distance between the hydrogen atoms adsorbed on the nearest Si sites is 3.59 Å. Thus, we take the halfway distance so that the flat sampling range is $0 \le b \le 1.80$ Å (i.e., $b_{max} = 1.80$ Å). In the collision with $b > 1.80$ Å, the gas atom is now in the interaction range of the adjacent surface site. If this site is covered, the gas atom is now in the interaction range of another adatom, in which case a different PES will have to be constructed. The initial conditions and numerical techniques needed in solving the equations of motion are given in ref 24.

Throughout this paper we have set the chain length of $(N+1) = 10$ after checking the dependence of energy transfer to the solid as a function of N. We define the reaction probability P at the gas and surface temperatures (T_g,T_s) as the ratio of the number of reactive trajectories N_R to the total number of trajectories sampled ($N_T = 30\,000$) over the entire range of

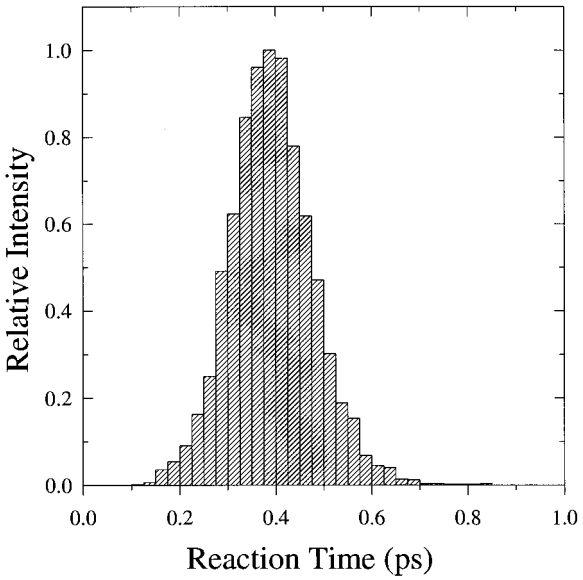

Figure 2. Distribution of reaction times at (1500, 300 K).

impact parameters. To define the reaction time, we first confirm the occurrence of a reactive event by following the trajectory for 50 ps, which is a sufficiently long time for the product HCl(g) to recede from the influence of surface interaction. Then we trace the reactive trajectory backward to find the time at which the H-to-Si separation has reached $r_{HSi,e} + 5.00$ Å, where $r_{HSi,e}$ is the equilibrium distance of the H−Si bond (1.514 Å). We define this time as the reaction time. At the thermal conditions of $(T_g,T_s) = (1500, 300$ K), 5255 trajectories of a total of 30 000 sampled over the entire range of impact parameters are found to be reactive (i.e., $P = 0.175$). Note that the gas temperature of 1500 K is known to be the typical experimental condition for producing chlorine atoms.[40] All of these reactive events occur on a subpicosecond time scale during which the adatom suffers only one impact with the surface, the ensemble-average of reaction times being 0.39 ps (see Figure 2). In such a direct collision, a significant amount of acceleration of the incident atom occurs both before and after impact, and when the atom turns the corner, it can then pick up the adatom, which is oscillating between two heavy atoms, i.e., Cl and Si. The reaction time decreases with increasing collision energy determined by the Maxwellian distribution at T_g. Especially short reaction times (∼0.2 ps) are found for the reactive events taking place in the high-energy tail of the distribution. At the present thermal condition, there is no evidence of the gas atom trapped on the surface. If there were such atoms with subsequent reactive events occurring on a long-time scale (>10 ps) long enough for trapped atoms to thermalize as in the case of O(g) + CO(ad)/Pt,[21] they would likely follow the precursor mechanism.[25,26] It should be important to note that in their study of the CO oxidation over a Ru surface, Peden and co-workers have considered the reaction to follow the ER mechanism if its reaction time is less than 10 ps.[41] Thus, we regard all these short-time direct-mode events in the present gas−adatom interaction to follow the ER mechanism, in which the incident atom cannot accommodate to the surface temperature.

Figure 3a shows a moderate dependence of the reaction probability on surface temperature. At a gas temperature of 1500 K, the probability increases slowly from 0.078 at $T_s = 0$ K to 0.240 at $T_s = 700$ K. These probabilities are significantly higher than those of the related reaction H(g) + H(ad)/Si or H(g) + Cl(ad)/Si. For example, at the thermal conditions of (1800, 300 K), the probability of H_2 formation in H(g) + H(ad)/Si is 0.11.[4]

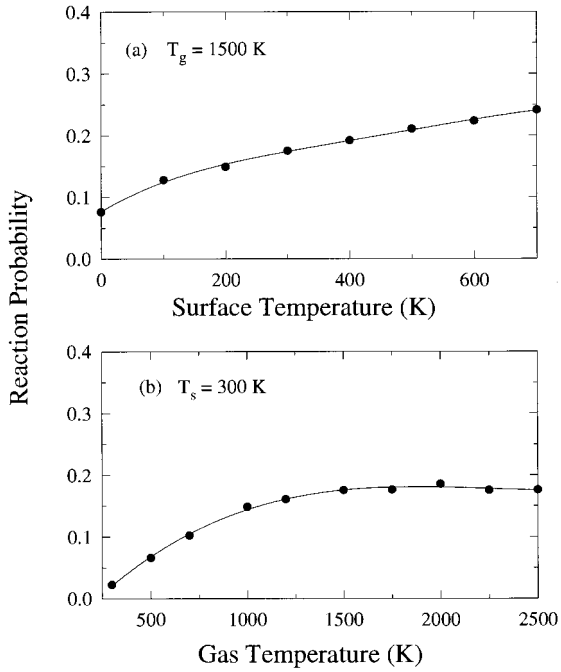

Figure 3. Temperature dependence of reaction probabilities: (a) dependence on the surface temperature for the gas temperature fixed at 1500 K; (b) dependence on the gas temperature for the surface temperature fixed at 300 K.

At (1500, 300 K), the probability of HCl formation in H(g) + Cl(ad)/Si is 0.099,[24] whereas that in the present reaction is 0.179, which is nearly twice the latter value, indicating an easier abstraction of the lighter hydrogen atom by the heavier chlorine atom. As shown in Figure 3b, the dependence of the reaction probability on T_g is significant at lower temperatures. At $T_s = 300$ K, there is a rather strong rise of P when the gas temperature is raised from 300 K to about 1000 K, but above the latter temperature the reaction probability remains nearly constant (∼0.18). The rise is a result of the incident atoms having greater collision energies according to the Maxwellian distribution. Since the barrier height is very small (∼0.14 eV), a further increase in T_g (or E) does not affect the extent of reaction significantly, since the collision energy in most of the ER reactive events has already surpassed the barrier height. Throughout the following sections, we consider the reaction to take place at the thermal condition of (1500, 300 K).

We define the opacity function $P(b)$ as the fraction of collisions with impact parameter b that lead to reaction (see Figure 4a). To determine this function, we count all reactive trajectories in intervals of $b = 0.050$ Å and divide the number of such trajectories $N_R(b)$ by the number of trajectories $N(b)$ sampled in the interval. For example, the number of trajectories sampled between $b = 0$ and 0.050 Å is $N(b) = 833$, of which 123 are reactive. Then the ratio $123/833 = 0.148$ is considered to be $P(b)$ at the midpoint of 0.025 Å. Note that the probability P defined above is a total probability expressed as the ratio of the total number of reactive trajectories $N_R = \sum N_R(b)$ to all trajectories sampled $N_T = 30\,000$ over the entire b range of $0-b_{max}$. As shown in Figure 4a, $P(b)$ is small in $b \cong 0$ collisions and then takes the maximum value near $b = 0.7$, after which it rapidly decreases as the impact parameter increases. Beyond $b = 1.5$ Å, the reaction ceases. The total reaction cross section calculated from the expression

$$\sigma = 2\pi \int_0^{b_{max}} P(b) b \, db$$

is 1.19 Å^2.

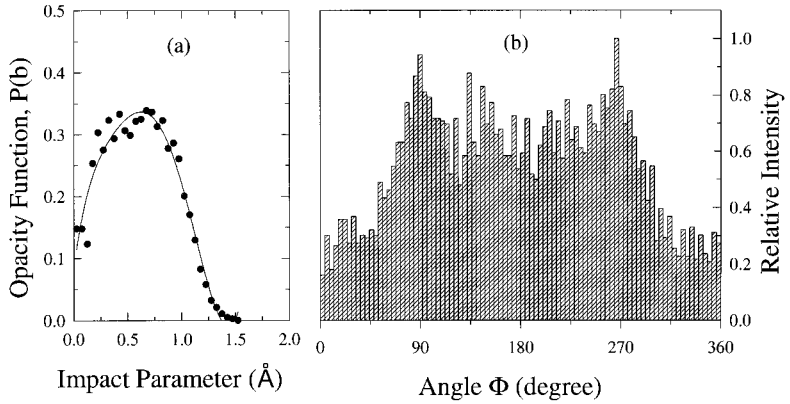

Figure 4. (a) Dependence of the opacity function on the impact parameter at (1500, 300 K). (b) Distribution of the azimuthal angle Φ of the incident atom leading to reaction at (1500, 300 K).

Since the nearest H−H distance in a highly covered case is 3.59 Å, we can consider a cylindrical region of the radius $^1/_2$(3.59 Å) = 1.80 Å around the adatom to be an interesting region for the occurrence of reactive events. The equilibrium HCl bond distance is 1.274 Å, so the height of the cylindrical region from the adatom cannot be significantly higher than this distance. A sharp decrease of $P(b)$ near the impact parameter corresponding to this bond distance seen in Figure 4a clearly indicates the difficulty experienced by the incident gas atom in abstracting the adatom when the impact parameter is near or greater than the HCl bond distance. The product HCl formed near the upper limit of b comes from those gas atoms approached near the surface at large b (i.e., near the bottom of the cylinder). Such gas atoms rarely form HCl, since they are bounced back by the repulsive energy of the surface atoms. Thus, the occurrence of reactive events in the range of $0 \leq b \leq 1.5$ Å, peaking near 0.5 Å, indicates that the events are confined to the neighborhood of the adatom site and are independent of the gas−next-nearest-adatom interaction in the case of high surface coverage. Such localized reactivity has been observed in other systems such as the hydrogen abstraction reaction on silicon by the gas-phase atomic hydrogen (H or D).[9] In the present model, we define $\Phi = 0$ in the direction where the adatom is tilted, and the origin of Φ to be the point on the surface where the surface normal axis meets the adatom. The initial value of Φ is selected randomly between 0 and 2π, and Figure 4b shows the distribution of this angle for reactive events. The distribution indicates a greater number of reactive events occurring between 90 and 270°. Since the adatom is tilted by 20.6°, the distance between this atom and the axis normal to the 0th Si atom is 1.51 sin α = 0.53 Å. Thus, the tilting exposes the five surface atoms of the second and third quadrants to the incident gas atom that is loosely bound to the adatom on the 0th silicon during the interaction. We expect the openness of this region to steer efficiently the gas atom to stay bound at the adatom site, thus enhancing the occurrence of reaction. Such steering is less effective in the first and fourth quadrants because the tilting causes the region to be less open to the incident atom. Consequently, the probability of the incident gas atom reacting with the adatom is greater when it approaches the second and third quadrants around the 0th Si atom (i.e., between 90 and 270°).

To present a clearer picture of localized reactive events occurring in the vicinity of adatom sites and the Φ dependence of such reactive events, we consider that all nine surface sites including the 0th Si site are covered by adatoms and we repeat the calculation for each adatom. Figure 5 shows the distribution of reaction impacts around each adatom site on the nine Si-atom surface. The numbering corresponds to the position of each Si atom along the symmetric dimer rows shown in Figure 1. Here, the numbering zero represents the 0th Si atom mentioned above. The equilibrium distance between nearest adatoms on a given dimer is 3.591 Å, whereas the Si−Si distance is 2.524 Å.[32] The nearest adatom−adatom distance between two nearby dimer rows is 4.086 Å (see Figure 5). In a given row, the nearest dimer−dimer distance is 3.866 Å. The radius of the circular region for reactive events around each adatom site is much shorter than these interatomic distances, and the plot clearly shows strong localization of reactive events in the neighborhood of the target atom. Around each adatom site there is a higher concentration of reactive events in half the region opposite the tilted adatom (e.g., the second and third quadrants of the 0th Si site). Note that the adatom is tilted in the $\Phi = 0°$ direction (i.e., the right-hand side) by 20.6° in the 0th, 1st, and 5th Si sites as mentioned above; their distributions of reactive impacts are essentially identical to one another. However, in the 2nd, 3rd, and 4th cases, the adatom is tilted in the $\Phi = 180°$ direction (i.e., the left-hand side), and the distribution is nearly an image of the 0th (as well as 1st and 5th) Si case.

The dependence of HCl vibrational energy $E_{vib,HCl}$ on the impact parameter presented in Figure 6a indicates the occurrence of significant vibrational excitation of product HCl in nonzero-impact parameter collisions. The general features of the plot are that the number of reactive events is small in $b \cong 0$ collisions as noted above (also see Figure 4a) and the extent of vibrational excitation decreases as the impact parameter increases toward 1.5 Å. Figure 6b indicates that the vibrational population distribution is non-Boltzmann, with the maximum appearing near the vibrational energy of 0.4 eV. From the eigenvalue expression $E_{vib}(v_{HCl}) = hc\omega_e(v_{HCl} + {}^1/_2) - hc\omega_e x_e(v_{HCl} + {}^1/_2)^2$ with $\omega_e = 2990.95$ cm^{-1}, $\omega_e x_e = 52.82$ cm^{-1},[33] we find the vibrational energies 0.185, 0.542, 0.886, and 1.218 eV for $v_{HCl} = 0$, 1, 2 and 3, respectively. The comparison of these energies with the energy scale used in Figure 6b indicates that about 40% of the product molecules have their vibrational energies close to $v = 1$. Since $D^0_{0,HSi}$ is 3.50 eV and $D^0_{0,ClH} = 4.434$ eV, the reaction exothermicity and the initial collision energy are large enough to produce such moderately excited molecules. To mimic the quantum vibrational distribution, we use a binning procedure of assigning quantum number v_{HCl} corresponding to the calculated vibrational energy through the relation $v_{HCl} = \text{int}[E_{vib,HCl}/E_{vib}(v_{HCl})]$. Using this procedure, we find that of a total of 5255 reactive trajectories, 2630 belong to $v_{HCl} = 0$, 2419 to $v_{HCl} = 1$, 203 to $v_{HCl} = 2$, and 3 to $v_{HCl} = 3$. That is, the intensity ratio of $v_{HCl} = 1$ to $v_{HCl} = 0$ is 0.92, which is far

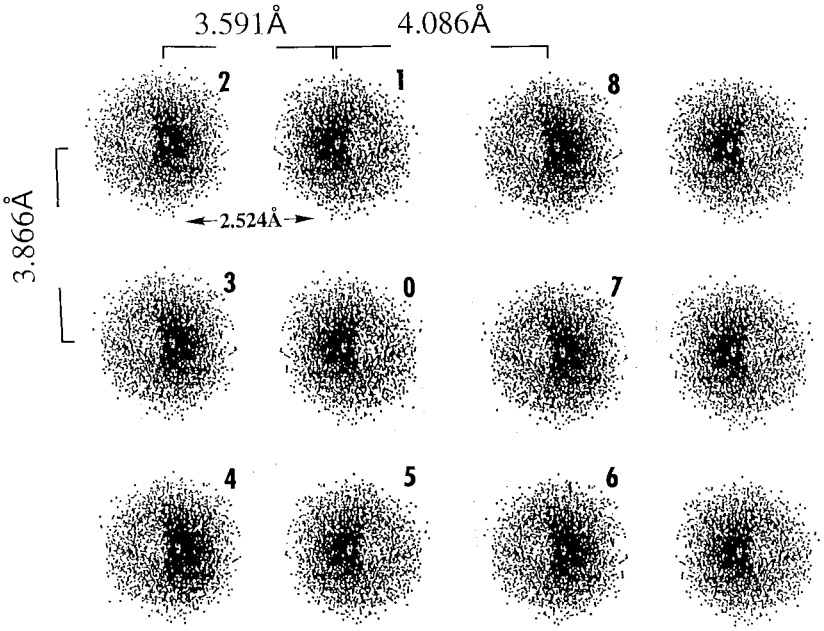

Figure 5. Location of reactive events around the adatom site. The reaction on nine adatom sites belonging to three dimers of the left-hand-side symmetric row (see 0, 1, ..., 5) and one-half of the nearby row (see 6, 7, 8) was considered at (1500, 300 K).

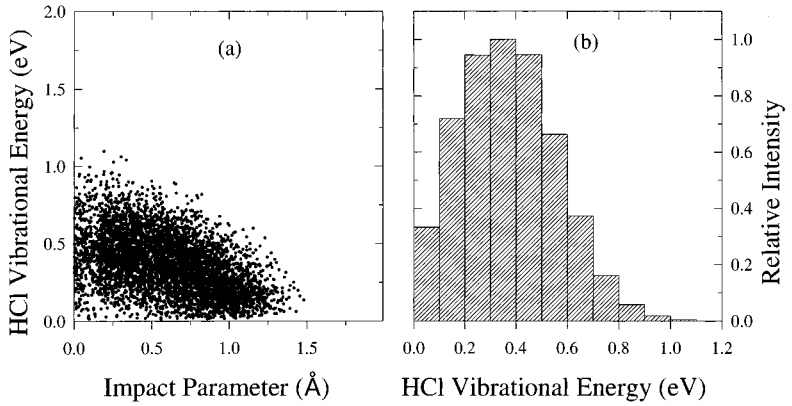

Figure 6. Distribution of the vibrational energy at (1500, 300 K): (a) dependence of the vibrational energy on the impact parameter; (b) vibrational population distribution.

greater than that predicted by the Boltzmann distribution even at a temperature as high as $T_g = 1500$ K. At this temperature, the Boltzmann distribution for the fraction of molecules in the ith energy level,

$$f_i = e^{-i\hbar\omega_{HCl}/(kT)} / \sum_{i=0}^{\infty} e^{-i\hbar\omega_{HCl}/(kT)}$$

where $i = v_{HCl}$, gives the corresponding intensity ratio as low as 0.053.

The amount of energy deposited in the translational motion of HCl is somewhat larger than the vibrational energy (compare Figures 6a and 7a). The ensemble-averaged translational energy is 0.434 eV, whereas the ensemble average of the vibrational energies displayed in Figure 6a is 0.371 eV. Figure 7a shows that some molecules recede from the surface with a translational energy larger than 1 eV, clearly indicating high translational excitation. This figure also shows the diminished number of reactive events with translational energy less than about 0.2 eV. In this case, more energy is deposited in the vibrational motion. Thus, such vibrationally excited molecules leave the surface more slowly. Figure 7b shows a time-of-flight distribution of product molecules along the fitted curve. The points are obtained by collecting molecules reaching the "reaction chamber-to-detector" distance of 30 cm. A smooth distribution of product velocities indicates the occurrence of a single type of reactive collision, namely, the direct-mode collision. The distribution fits well with a velocity function of the form

$$f(v) = Av^3 e^{-(v-v_0)^2/\alpha^2}$$

with $v_0 = 1550$ m/s and $\alpha = 329$ m/s, where A is the normalization constant. These v_0 and α values indicate that the velocity distribution is highly non-Boltzmann with a mean energy ($^1/_2 m_{HCl} v_0^2 = 0.448$ eV) far in excess of $kT_s = 0.026$ eV or even $kT_g = 0.129$ eV. The most probable speed determined from the distribution function is 1512 m/s, which corresponds to 0.426 eV. Note that the mean energy calculated from the time-of-flight distribution is very close to the ensemble-averaged translational energy of 0.434 eV mentioned above.

It is interesting to compare the energy distribution in the present reaction Cl(g) + H(ad)/Si with that of the related reaction H(g) + Cl(ad)/Si, where the light atom interacts with the heavy atoms (**L** + **HH**). Both reactions are driven by reaction exothermicities of similar magnitude (0.8−1.0 eV). However, the two reactions have very different mass distributions, which

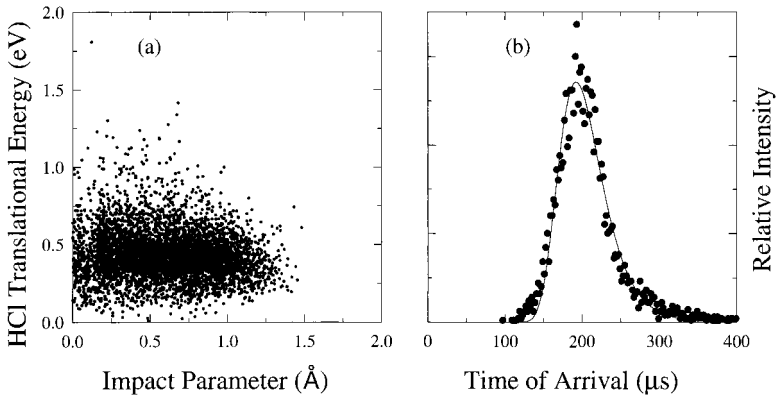

Figure 7. Distribution of the translational energy at (1500, 300 K): (a) dependence of the translational energy on the impact parameter; (b) time-of-flight distribution for HCl from the surface.

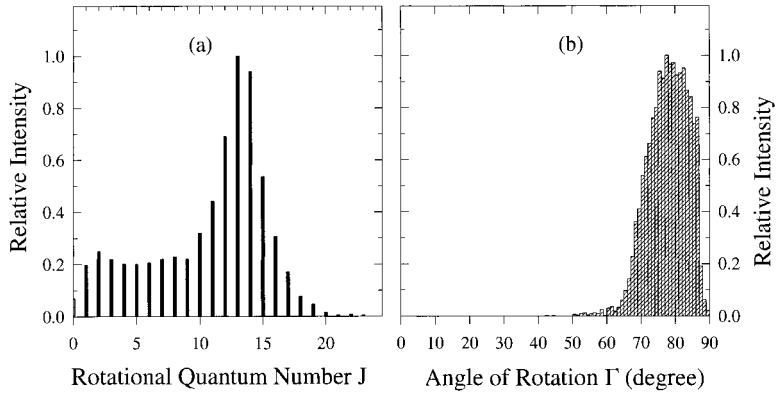

Figure 8. (a) Relative intensity of the rotational population distribution at (1500, 300 K). (b) Distribution of the angle between the axis of rotation and the surface normal Γ.

lead to unusual kinematics directly affecting the outcome of the product energy distribution in each reaction. As shown in Figure 6b, the vibrational population does not follow the Boltzmann distribution f_i, and this population distribution is fundamentally different from that of the H(g) + Cl(ad)/Si reaction, where the distribution is statistical.[24] In the present reaction, the heavy incident atom favors energy deposit in the vibrational motion of the HCl molecule, thus producing a vibrational distribution which is non-Boltzmann. In the present reaction (**H** + **LH**), the light adatom moves back and forth between the two heavy atoms, efficiently transferring energy between the **H**···**L** and **L**···**H** bonds with most of the available energy in their vibrational motions. In this reaction, therefore, the reaction probability is significantly larger than that in the **L** + **HH** case, where the heavy adatom blocks energy flow from **L**···**H** to **H**−**H**. The occurrence of such energy flow blockage by heavy atoms has already been reported by others.[42−45] Furthermore, the energy that has managed to accumulate in the **H**−**H** bond can dissipate more readily to the surface than that in the **H** + **LH** case, thus leading to less energy accumulation in the **H**−**H** bond. Therefore, different dynamic features during the course of reaction affect seriously the outcome of the reactions.

The amount of energy taken up by the rotational motion of the HCl molecule is small, in contrast to the translational and vibrational motions. Here, the rotational energy is $E_{HCl,rot} = L^2/(2\mu_{HCl}r_{HCl}^2)$, where the angular momentum $L = \mu_{HCl}(z\dot{\rho} - \rho\dot{z})$ with the corresponding quantum number $J = L/\hbar$. The ensemble-averaged rotational energy is only 0.210 eV. As in the vibrational case discussed above, we apply the binning procedure of assigning rotational quantum number J_{HCl} corresponding to the calculated rotational energy $E_{HCl,rot}$ through the relation J_{HCl} = **int**[$E_{HCl,rot}/E_{rot}(J_{HCl})$], where $E_{rot}(J_{HCl}) = J_{HCl}\ (J_{HCl} + 1)\hbar^2/(2I_{HCl}kT)$. The relative intensity of the rotational population distribution shown in Figure 8a indicates a characteristic of the bimodal form of the intensity. The main peak appears near J = 13, which deviates significantly from the Boltzmann distribution. The maximum obtained from the Boltzmann distribution $J_{max} = {}^1/_2[(2kT/\bar{B})^{1/2} - 1]$ with $\bar{B} = 10.58$ cm^{-1} at 1500 K is 7. Although the intensity varies slightly below J = 10, there appears to be another mode with the intensity peaking near J = 2. The present analysis reveals the interesting case of the rotational alignment of HCl at the instant of desorption from the surface. To examine this aspect, we have calculated the angle between the axis of rotation of HCl and the surface normal, Γ, when the Cl atom turns the corner with H and begins the journey outward. The relative intensity plotted in Figure 8b is for the ensemble of all reactive events. The angles are heavily distributed near 90°, where the rotational axis is parallel to the surface. That is, HCl product molecules leave the surface in a cartwheel-like rotation. As noted above, the collinear configuration for the tilted Si···H with Cl occurs near b = 0.5 Å, where the energy release at the instant of dissociation will tend to propel H upward, causing the atom in HCl to rotate clockwise. All those gas atoms steered to remain near the tilted adatom by the surface atoms of the second and third quadrants are likely to undergo the same type of rotation when they react with Cl in a nonzero-b collision. In the distribution presented in Figure 5, therefore, HCl formed on the right-hand-side Si (i.e., 0th, 1st, 5th) rotates clockwise, whereas that formed on the left-hand-side Si (i.e., 2nd, 3rd, 4th) rotates counterclockwise. Thus, in the narrow range of the dimer strand measuring about 8 Å (i.e., 3.591 Å + 4.086 Å), there can be two distinct directions for the rotational motion of the HCl molecules produced on

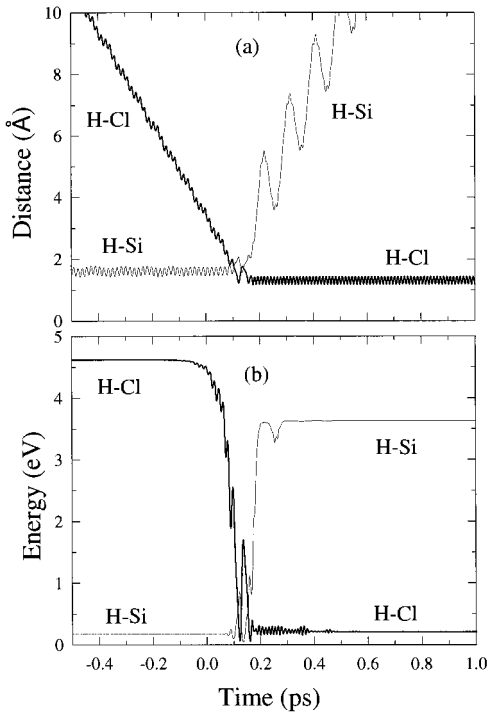

Figure 9. Dynamics of the representative trajectory at (1500, 300 K): (a) time evolution of the Cl-to-H and H-to-Si distances; (b) time evolution of the Cl-to-H interaction energy and the H−Si vibrational energy.

the silicon surface. It should be both interesting and important to test this prediction of circular polarization experimentally. We note that there are no desorbing molecules rotating like helicopters.

The amount of energy transfer to the silicon surface is small because of the large difference between the masses of H and Si. The reaction taking place at the thermal conditions (1500, 0 K) gives a much clearer picture of energy transfer to the surface as the surface atoms are initially at rest, and there are no systematic or random forces exerted by the heat bath. In this case the entire energy that has propagated from the adatom−surface vibration to the vibration of the 0th atom of the *N*-atom chain has dissipated into the chain and then into the heat bath. There is no flow of energy back from the heat bath. Thus, we can determine the energy transfer to the solid unequivocally. At these thermal conditions, the ensemble-average of energy transfer to the surface is 0.024 eV.

Finally, we look into several important aspects of the dynamics of this reaction. As noted in the early part of this section, all reactive events of the 30 000 trajectories sampled occur on the subpicosecond time scale, and the vibrational population is non-Boltzmann. Figure 9a shows the H−Si and H−Cl (or Cl−H) distances for the representative trajectory. Before collision, the H−Si bond undergoes a highly regular vibration at 2093 cm^{-1}. The Cl-to-H distance also oscillates by the same frequency, since the adatom vibration affects the Cl-to-H distance. Near $t = 0.1$ ps it suffers impact with the adatom, forming HCl. The formation is clearly seen from the highly organized vibrational motion of the H−Cl distance, as well as from the divergence of the H−Si distance. The large-amplitude oscillatory motion of H−Si after the impact represents the rotation of HCl as it recedes from the surface. For this representative case, the rotational period is 0.11 ps, which is nearly 9 times the vibrational period. The Cl-to-H interaction energy begins with 4.62 eV, which begins to decrease near $t = -0.10$ ps, which can be identified as the start of interaction (see Figure 9b). It rapidly decreases near $t = 0$, reaching near zero, while the H−Si vibrational energy rapidly rises to the H−Si dissociation threshold of 3.63 eV. Figure 9b clearly shows an efficient exchange flow of energy from the Cl-to-H interaction to the H−Si vibration in a brief period of about 0.3 ps. The decrease of the Cl-to-H interaction occurs stepwise. In the present mass distribution of **H + LH**, the light atom oscillates between two heavy atoms, pumping energy from Cl−H to H−Si. Thus, the incident atom initially trapped in the upper region of the potential well rapidly cascades down the well through ladder-climbing (or declimbing) processes in which the Cl-to-H interaction loses its energy in a series of small steps. In contrast, in the **L + HH** case (e.g., the H + Cl/Si reaction), the process of deactivation occurs in a single-step process.[24] Figure 9b also shows that the vibrational energy of HCl finally settles at a constant value of 0.209 eV at $t = +0.48$ ps. Since impact occurs at $t = +0.12$ ps, the reaction time for this representative event can be determined as 0.36 ps. As noted above, the collision begins at $t = -0.10$ ps, so the duration of collision can be determined as 0.46 ps.

IV. Concluding Comments

The gas−surface reaction Cl(g) + H(g)/Si → HCl(g) + Si through the Eley−Rideal mechanism is shown to be efficient in the gas temperature range 1000−2500 K on a silicon surface maintained at 300 K. All reactive events occur on the subpicosecond time scale, following the direct-mode collision between the incident gas atom and the adatom. The occurrence of these reactive events is concentrated in the immediate neighborhood of the adatom, and there is no evidence of product molecules trapped on the surface. The largest fraction of the reaction exothermicity is deposited in the product translation, followed by vibration and rotation. These product energy distributions are found to be non-Boltzmann. The amount of the reaction energy dissipated to the surface is small. The product molecules rotate cartwheel-like when they leave the surface.

Acknowledgment. The computational part of this research was supported by a NSF Advanced Computing Resources grant at the San Diego Supercomputing Center. W.K.K. and J.R. gratefully acknowledge the financial support from Chonnam National University.

References and Notes

(1) Bozso, F.; Avouris, P. *Appl. Phys. Lett.* **1988**, *53*, 1095.
(2) Cheng, C. C.; Lucas, S. R.; Gutleben, H.; Choyke, W. J.; Yates, J. T., Jr. *J. Am. Chem. Soc.* **1992**, *114*, 1249.
(3) Yates, J. T., Jr.; Cheng, C. C.; Gao, Q.; Choyke, W. J. *Surf. Sci. Rep.* **1993**, *19*, 79.
(4) Koleske, D. D.; Gates, S. M.; Jackson, B. *J. Chem. Phys.* **1994**, *101*, 3301.
(5) Waltenburg, H. N.; Yates, J. T., Jr. *Chem. Rev.* **1995**, *95*, 1589.
(6) Doren, D. J. *Adv. Chem. Phys.* **1996**, *95*, 1.
(7) Buntin, S. A. *J. Chem. Phys.* **1998**, *108*, 1601.
(8) Hall, R. I.; Cadez, I.; Landau, M.; Pichou, F.; Schermann, C. *Phys. Rev. Lett.* **1988**, *60* 337.
(9) Eenshuistra, P. J.; Bonnie, J. H. M.; Los, J.; Hopman, H. J. *Phys. Rev. Lett.* **1988**, *60*, 341.
(10) Kuipers, E. W.; Vardi, A.; Danon, A.; Amirav, A. *Phys. Rev. Lett.* **1991**, *66*, 116.
(11) Rettner, C. T. *Phys. Rev. Lett.* **1992**, *69*, 383.
(12) Schermann, C.; Pichou, F.; Landau, M.; Cadez, I.; Hall, R. I. *J. Chem. Phys.* **1994**, *101*, 8152.
(13) Tully, J. C. *J. Chem. Phys.* **1980**, *73*, 6333.
(14) Kratzer, P.; Brenig, W. *Surf. Sci.* **1991**, *254*, 275.
(15) Kratzer, P. *J. Chem. Phys.* **1997**, *106*, 6752.
(16) Jackson, B.; Persson, M. *J. Chem. Phys.* **1992**, *96*, 2378.
(17) Jackson, B.; Persson, M. *Surf. Sci.* **1992**, *269*, 195.

(18) Persson, M.; Jackson, B. *J. Chem. Phys.* **1995**, *102*, 1078.
(19) Shin, H. K. *J. Chem. Phys*. **1992**, *96*, 3330.
(20) Shin, H. K. *Chem. Phys. Lett*. **1995**, *244*, 235.
(21) Ree, J.; Kim, Y. H.; Shin, H. K. *J. Chem. Phys.* **1996**, *104*, 742.
(22) Ree, J.; Kim, Y. H.; Shin, H. K. *J. Phys. Chem. A* **1997**, *101*, 4523.
(23) Shin, H. K. *J. Phys. Chem*. **1998**, *102*, 2372.
(24) Kim, Y. H.; Ree, J.; Shin, H. K. *J. Chem. Phys*. **1998**, *108*, 9821.
(25) Harris, J.; Kasemo, B. *Surf. Sci*. **1981**, *105*, L281.
(26) Harris, J.; Kasemo, B.; Törnqvist, E. *Surf. Sci*. **1981**, *105*, L288.
(27) Kastanas, G. N.; Koel, B. E. *Appl. Surf. Sci.*. **1993**, *64*, 235.
(28) Rettner, C. T. *J. Chem. Phys*. **1994**, *101*, 1529.
(29) Adelman, S. A. *J. Chem. Phys.* **1979**, *71*, 4471.
(30) Tully, J. C. *J. Chem. Phys.* **1980**, *73*, 1975.
(31) Gates, S. M.; Kunz, R. R.; Greenlief, C. M. *Surf. Sci*. **1989**, *207*, 364.
(32) Radeke, M. R.; Carter, E. A. *Phys. Rev B.* **1996**, *54*, 11803.
(33) Huber, K. P.; Herzberg, G. *Constants of Diatomic Molecules*; Van Nostrand Reinhold: New York, 1979.
(34) Van de Walle, C. G.; Street, R. A. *Phys. Rev. B* **1995**, *51*, 10615.
(35) Kratzer, P.; Hammer, B.; Norskov, J. K. *Phys. Rev. B* **1995**, *51*, 13432.
(36) Tully, J. C.; Chabal, Y. J.; Raghavachari, K.; Bowman, J. M.; Lucchese, R. R. *Phys. Rev. B* **1985**, *31*, 1184.
(37) Vidali, G.; Ihm, G.; Kim, H. Y.; Cole, M. W. *Surf. Sci. Rep*. **1991**, *12*, 133.
(38) Harris, J. In *Dynamics of Gas−Surface Interactions*; Rettner, C. T., Ashfold, M. N. R., Eds.; Royal Society of Chemistry, Thomas Graham House: Cambridge, England, 1991.
(39) Namiki, A.; Hayashi, H.; Ukai, Y.; Geuzebroek, F. H. *J. Chem. Phys*. **1995**, *102*, 9689.
(40) Struve, W. S.; Krenos, J. R.; McFadden, D. L.; Herschbach, D. R. *J. Chem. Phys*. **1975**, *62*, 404.
(41) Peden, C. H. F.; Goodman, D. W.; Weisel, M. D.; Hoffmann, F. M. *Surf. Sci*. **1991**, *253*, 44.
(42) Rogers, P. J.; Selco, J. I.; Rowland, F. S. *Chem. Phys. Lett.* **1983**, *97*, 313.
(43) Lopez, V.; Marcus, R. A. *Chem. Phys. Lett*. **1982**, *93*, 232.
(44) Uzer, T; Hynes, J. T. *J. Phys. Chem*. **1986**, *90*, 3524.
(45) Shin, H. K. *J. Chem. Phys*. **1989**, *91*, 929.